Bioorganic & Medicinal Chemistry 20 (2012) 4430–4436

Contents lists available at SciVerse ScienceDirect

Bioorganic & Medicinal Chemistry

journal homepage: www.elsevier.com/locate/bmc

Synthesis, biological evaluation and molecular docking studies of 3-(1,3-diphenyl-1*H*-pyrazol-4-yl)-*N*-phenylacrylamide derivatives as inhibitors of HDAC activity

Xi Li [a], Jia-Lin Liu [a], Xian-Hui Yang [a], Xiang Lu [a], Ting-Ting Zhao [a], Hai-Bin Gong [b,*], Hai-Liang Zhu [a,*]

[a] State Key Laboratory of Pharmaceutical Biotechnology, Nanjing University, Nanjing 210093, PR China
[b] Xuzhou Central Hospital, Xuzhou 221009, PR China

ARTICLE INFO

Article history:
Received 27 March 2012
Revised 14 May 2012
Accepted 14 May 2012
Available online 26 May 2012

Keywords:
3-(1,3-Diphenyl-1*H*-pyrazol-4-yl)-*N*-phenylacrylamide derivatives
Histone deacetylase (HDAC)
Structure–activity relationship
Molecular docking

ABSTRACT

In present study, a series of 3-(1,3-diphenyl-1*H*-pyrazol-4-yl)-*N*-phenylacrylamide derivatives (**5a–8d**) were designed, synthesized, and evaluated for HDAC inhibition and tumor cell antiproliferation. All of these compounds are reported for the first time, the chemical structures of these compounds were confirmed by means of ^{1}H NMR, ESI-MS and elemental analyzes. Among the compounds, compound **8c** showed the most potent biological activity against HCT116 cancer cell line (IC_{50} of 0.42 ± 0.02 μM for HDAC-1 and IC_{50} = 0.62 ± 0.02 for HCT116). Docking simulation was performed to position compound **8c** into the HDAC active site to determine the probable binding model. The results of antiproliferative assay and western-blot demonstrated that compound **8c** with potent inhibitory activity in tumor growth inhibition may be a potential anticancer agent against HCT116 cancer cell.

1. Introduction

The role of gene regulation by physical alterations of either DNA or the structural components of chromatin has recently been highlighted as a major process in neoplastic transformation and maintenance of the malignant phenotype.[1] The reversible acetylation of -*N*-acetyl groups of lysine residues, in the N-terminal tails of core histones, plays a critical role in the regulation of gene expression by altering the accessibility of transcriptional factors to DNA via conformational changes in the structure of the nucleosome.[2–4] This restructuring of chromatin is regulated by the balance of histone acetyl transferase (HAT) and histone deacetylase (HDAC) activity.[5,6] Perturbations of this balance have been linked to gene expression, the inappropriate recruitment of HDACs provides at least one mechanism by which oncogenes can alter gene expression in favor of excessive proliferation.[7] Moreover, evidence demonstrates that inhibition of HDAC triggers growth arrest, differentiation, and/or apoptosis in many types of tumor cells by reactivating the transcription of a small number of genes.[8,9] These findings suggest that modulation of HDAC's function might be targeted for the prevention and/or therapeutic intervention of cancer. Based on pre-clinical findings, several HDAC inhibitors are presently in clinical trial for the treatment of a variety of haematological and solid tumors, including colon cancer.[10–12]

Till date, several structurally distinct compounds targeting HDAC enzyme have been reported, and with few exceptions, these can be divided into a few structural classes, including small-molecular hydroxmates, carboxylates, benzamides, electrophilic ketones and cyclic peptides.[13] Recent publication of the X-ray crystallography revealed that the structure of the HDAC active site is comprised of a tubular hydrophobic pocket and active site zinc.[14] A typical HDAC inhibitor includes three molecular fragments, namely, a metal-binding domain, which interacts with the active site, a linker domain, which occupies the channel, and a surface recognition domain, which interacts with residues on the rim of the active site.[15,16] Capitalizing on published SAR, we designed and synthesized a variety of compounds building off of an acylamide template, with the presumption that the carbonyl-oxygen group coordinate to the active site zinc and the double bond acts as a hydrocarbon linker to fill out the narrow tunnel.[17] On the other hand, acylamide is an important pharmacophore of natural products and the synthetic precursors to various drugs.[18,19] On that basis, a double bond was introduced into the amide moiety to construct an α,β-unsaturated acylamide, with the reasoning that α,β-unsaturated enones could also react with the nuclephilic groups of residues in HDAC domain.[20] Furthermore, structure-guided designs suggested that a substituted five-membered ring projecting from the 3-position of *N*-cinnamamide would best facilitate productive interaction between a binding moiety and

* Corresponding authors. Tel.: +86 25 8359 2572; fax: +86 25 8359 2672.
E-mail addresses: ghbxzh@yahoo.com.cn (H.-B. Gong), zhuhl@nju.edu.cn (H.-L. Zhu).

0968-0896/$ - see front matter © 2012 Elsevier Ltd. All rights reserved.
http://dx.doi.org/10.1016/j.bmc.2012.05.031

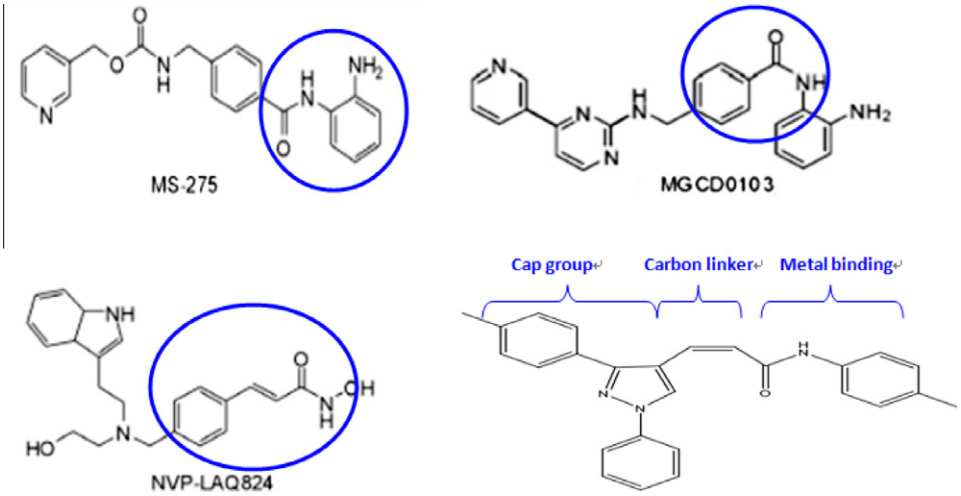

Figure 1. Three main types of scaffold found in reported HDAC inhibitors. Pharmacophoric features of HDAC inhibitors in the title compounds.

the protein surface.[21] As is known, pyrazole derivatives are a very interesting class of heterocyclic compounds that have remarkable pharmacological activities as antibacterial–antifungal, tumor necrosis inhibitor and antiangiogenic agent.[22–26] Given the pharmacological function of pyrazole derivatives, *N*-arylpyrazole is chosen as a surface recognition domain to interact with the amino acids near the entrance of the active site. In an effort to enhance the affinity and selective of HDAC, we synthesized a series of compounds building off of an acylamide template combined with pyrazole considering that they might exhibit synergistic effect in anticancer activities by the inhibition against HDAC (Fig. 1).

In this paper, we synthesized a series of 3-(1,3-diphenyl-1*H*-pyrazol-4-yl)-*N*-phenylacrylamid, in an attempt to extend previous research on the benzamide class of HDAC inhibitors. Herein, in continuation to further our research on antitumor compounds with HDAC structure inhibitory activity, advances have been made in designing new phenylacrylamid derivatives, which share the core template with the benzamide class can be as developments to enrich and optimize HDAC inhibition activity. The anticancer activities of the synthesized compounds were evaluated in HCT116 and the preliminary mechanism of the active compound was further examined by docking study.

2. Results and discussion

2.1. Chemistry

The synthetic route of the 3-(1,3-diphenyl-1*H*-pyrazol-4-yl)-*N*-phenylacrylami derivatives is outlined in Scheme 1. As reported,[27] the synthesis of 3-(1,3-diphenyl-1*H*-pyrazol-4-yl)-*N*-phenylacrylamid begins with the interaction of substituted 1,3-diphenyl-1*H*-pyrazole-4-acrylic acid and substituted anilines with the help of DMAP and K_2CO_3 in anhydrous methylene dichloride to give the desired compounds. These compounds are all reported for the first

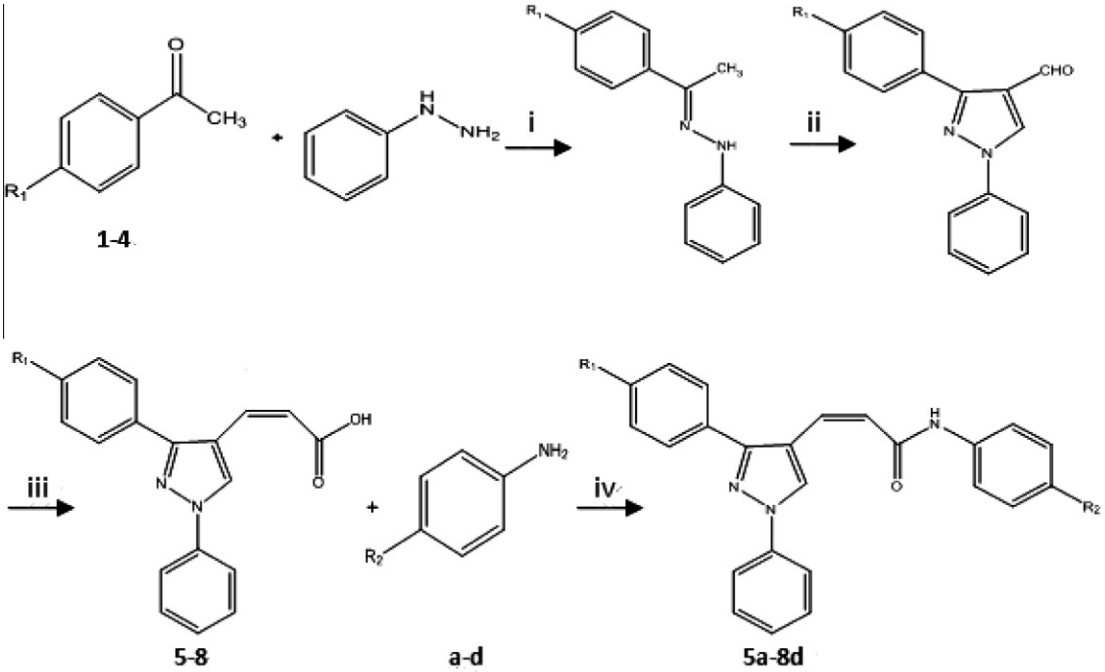

Scheme 1. General synthesis of 3-(1,3-diphenyl-1*H*-pyrazol-4-yl)-*N*-phenylacrylamid derivates derivatives (**5a**–**8d**). Reagents and conditions: (i) ethanol, 50–60 °C, 3 h; (ii) DMF, $POCl_3$, 50–60 °C, 5 h; (iii) piperidine/$CH_2(COOH)_2$,40–50 °C, 5 h;(iv)DMAP, K_2CO_3, dichloromethane, 50–60 °C, 12 h.

Table 1
Structure of compounds **5a–8d**

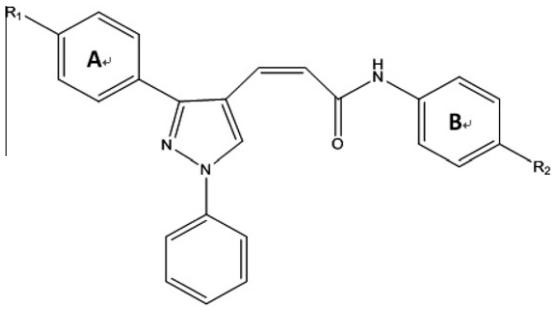

Compd	R_1	R_2	Compd	R_1	R_2
5a	Me	H	**7a**	Br	H
5b	Me	Cl	**7b**	Br	Cl
5c	Me	Br	**7c**	Br	Br
5d	OMe	OMe	**7d**	Br	OMe
6a	OMe	H	**8a**	NO_2	H
6b	OMe	Cl	**8b**	NO_2	Cl
6c	OMe	Br	**8c**	NO_2	Br
6d	OMe	OMe	**8d**	NO_2	OMe

time. All of the synthesized compounds **5a–8d** (Table 1) gave satisfactory elementary analytical and spectroscopic data. ^{1}H NMR and ESI-MS spectra were consistent with the assigned structures.

2.2. Bioactivity

To test the anticancer activities of the synthesized compounds, we evaluated antiproliferative activities of compounds **5a–8d** against HCT116 and A549 cells. The results were summarized in Table 2. As illustrated in Table 2, with few exception, the active analogs showed a remarkable potential antitumor activity, suggesting that 1*H*-pyrazole-4-phenylacrylamid pharmacophore significantly enhanced anticancer potency. For the given compounds, it was observed that compound **8c** showed the most potent biological activity (IC_{50} = 0.62 ± 0.02 for HCT116 and IC_{50} = 3.71 ± 0.12 for A549).

From the results listed in Table 2 we can arrive at the conclusion that the activity of the tested compounds may be correlated to structure variation and modifications. By investigating the variation in selectivity of the tested compounds over the two cell lines, it was obviously revealed that different substitutes on the A-ring determine the primary order of potency. A comparison of the *para*-substituents on the A-ring demonstrated that NO_2 group have dramatically improved antiproliferative activity, with the presumption that NO_2 group at the *para*-position of ring A may bind potently into HDAC through π-cation interaction. In addition, *para*-OMe group substituent is also well tolerated in this position, suggesting that *para*-substituents of A-ring play a key role in reacting with the function groups of residues in HDAC domain. However, Me and Br group showed minimal effects for the reason that they may lack chemical bonds with HDAC. In the case of constant A-ring substituents, change of substituents on the B-ring could also affect the activities of these compounds. Among the compounds, the compounds with Br and Cl group as electron-withdrawing substituents on ring B are of better antitumor activity comparing to those with electron-donating, the potency of *para*-substituents on the B-ring is ordered as: Br > Cl > H > MeO, followed that **5d,7d** are not tolerated. Among all the compounds, **8c** with *para*-NO_2 group on the A-ring and *para*-Br on the B-ring, respectively, led to a noteworthy best activity.

Table 2
Inhibition (IC_{50}) of HCT116, A549 cells proliferation and inhibition of HDAC-1, HDAC-2 by compounds **5a–8d**

Compd	IC_{50} ± SD (μM)			
	HCT116[a]	A549[a]	HDAC-1[b]	HDAC-2[b]
5a	10.36 ± 0.56	16.13 ± 0.72	4.06 ± 0.10	8.75 ± 0.67
5b	7.65 ± 0.63	15.41 ± 0.89	3.65 ± 0.13	5.86 ± 0.46
5c	7.16 ± 0.91	11.79 ± 0.83	3.33 ± 0.21	5.02 ± 0.38
5d	9.81 ± 0.14	>20	4.05 ± 0.14	6.45 ± 0.33
6a	2.09 ± 0.12	9.85 ± 0.65	1.76 ± 0.12	2.67 ± 0.14
6b	1.56 ± 0.08	8.04 ± 0.79	1.09 ± 0.08	2.36 ± 0.12
6c	1.53 ± 0.06	7.47 ± 0.74	1.05 ± 0.06	2.17 ± 0.10
6d	2.12 ± 0.10	8.59 ± 1.07	1.73 ± 0.10	3.02 ± 0.45
7a	10.71 ± 1.03	>20	3.43 ± 0.13	6.52 ± 0.43
7b	8.37 ± 0.98	15.75 ± 0.91	2.98 ± 0.18	4.99 ± 0.28
7c	8.16 ± 0.79	12.18 ± 1.13	2.83 ± 0.09	4.87 ± 0.26
7d	9.69 ± 1.09	>20	3.31 ± 0.09	5.35 ± 0.27
8a	0.85 ± 0.03	5.18 ± 0.47	0.92 ± 0.03	1.15 ± 0.09
8b	0.64 ± 0.04	3.72 ± 0.16	0.46 ± 0.04	0.57 ± 0.04
8c	0.62 ± 0.02	3.71 ± 0.12	0.42 ± 0.02	0.55 ± 0.03
8d	1.08 ± 0.03	5.17 ± 0.64	1.02 ± 0.02	1.15 ± 0.08
MS-275	<0.10	<0.10	<0.10	<0.10

[a] Inhibition of the growth of tumor cell lines.
[b] Inhibition of HDAC.

On the basis of previous research, it is revealed that the class of benzamide HDAC inhibitors bore exclusively HDAC-1 and HDAC-2 inhibition.[17] To further examine whether the compounds inhibit HDAC, we screen compounds **5a–8d** against the HDAC-1 and HDAC-2. The results were summarized in Table 2. Most of the tested compounds displayed potent HDAC-1 and HDAC-2 inhibitory. Among them, compounds **8c** showed the most potent inhibitory with IC_{50} of 0.42 ± 0.02 μM against HDAC-1 and IC_{50} of 0.55 ± 0.03 μM against HDAC-2. The results of HDAC inhibitory activity of the tested compounds were corresponded to the structure relationships (SAR) of their antitumor activities. This demonstrated that the potent antitumor activities of the synthetic compounds were probably correlated to their HDAC inhibitory activities.

In an effort to study the preliminary mechanism of the compound with potent inhibitory activity, the Western-blot experiment was performed to assay the effect of compound **8c**. The Western-blot results were summarized in Figure 2. The result indicated that compound **8c** showed excellent HDAC inhibitory activity against HCT116.

In order to gain more insight into the potency of the studied compounds and guide further structure–activity relationship studies, we proceeded to examine the interaction of compound **8c** with human HDAC-2 crystal structure (3MAX.pdb). The molecular docking was performed by inserting compound **8c** into the active site of HDAC-2. All docking runs were applied LigandFit Dock protocol of Discovery Studio 3.1. The binding mode of compound **8c** and HDAC-2 were depicted in Figure 3a. All the amino acid residues which had interactions with HDAC-2 were exhibited in Figure 4. In the binding mode, compound **8c** is potently bound to the active site of HDAC-2 via hydrophobic interactions and binding is stabilized by a hydrogen bond and two π-cation interactions. The hydrogen atom of the amide group involved in a hydrogen bond

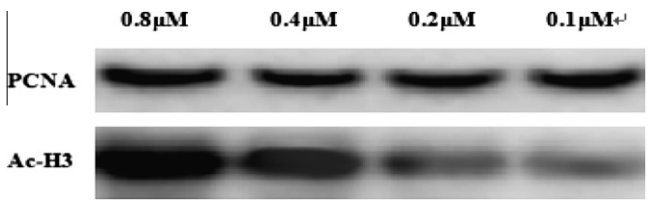

Figure 2. Compound **8c** was examined by western blotting. Data are representative of three independent experiments.

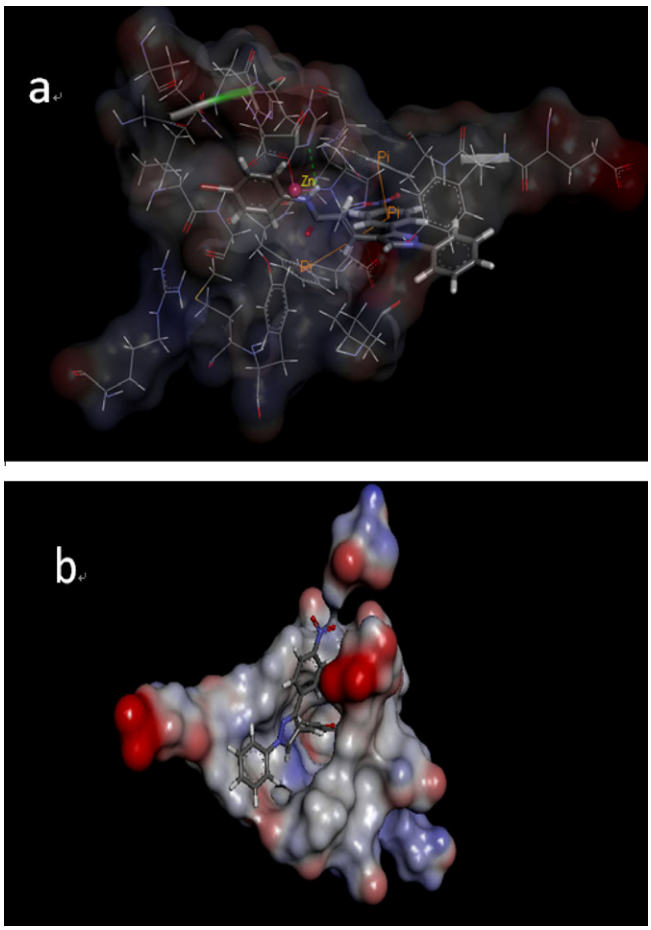

Figure 3. (a) Compound **8c** (colored by atom: carbons: gray; nitrogen: blue; oxygen: red) is bond into human HDAC-2(entry 3MAX in the Protein Data Bank). The dotted lines show the hydrogen bond and the yellow line show the π-cation interaction. (b) The surface model structure of compound **8c** binding model with HDAC-2 complex.

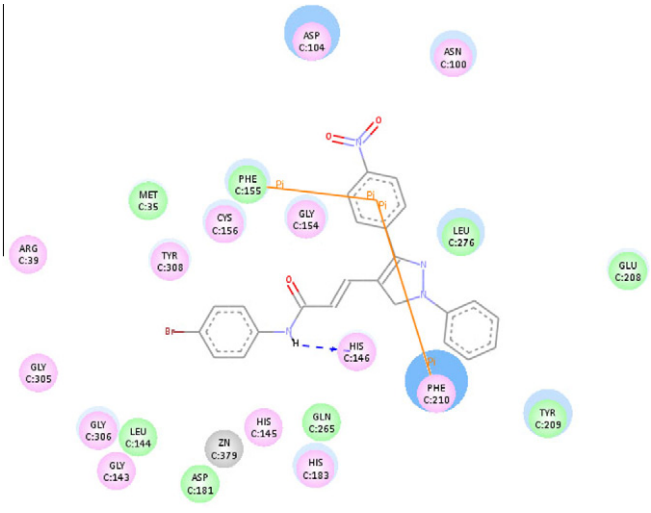

Figure 4. 2D Ligand interaction diagram of compound **8c** with HDAC-2 using Discovery Studio program with the essential amino acid residues at the binding site are tagged in circles. The purple circles show the amino acids which participate in hydrogen bonding, electrostatic or polar interactions and the green circles show the amino acids which participate in the Van der Waals interactions.

with the sidechain of His C:146 (bond length: 2.44 Å; bond angle: 107.5°), moreover, the nitrogen of the amide group chelates the zinc, in an attempt to access the pockt as deeply. On the other hand, the benzene ring with nitro moiety formed two π-cation interactions, respectively, with Phe C:155 (bond length: 6.36 Å) and Phe C:210 (bond length: 3.78 Å), Phe 155 and Phe 210 are part of the lipophilic tube, which leads from the surface to this machinery. The enzyme surface model was showed in Figure 3b, which revealed that the molecule was well embedded in the active pocket. This molecular docking result, along with the biological assay data, suggested that compound **8c** was a potential inhibitor of HDAC.

3. Conclusion

In this study, a series of 3-(1,3-diphenyl-1*H*-pyrazol-4-yl)-*N*-phenylacrylamid derivatives have been synthesized and evaluated for their antitumor activities. These compounds exhibited potent antiproliferative activities against HTC116 and HDAC inhibitory activities. Among all of the synthesized compounds, compound **8c** demonstrated the most potent inhibitory activity (IC_{50} of 0.42 ± 0.02 μM for HDAC-1 and IC_{50} of 0.55 ± 0.03 μM for HDAC-2). Antiproliferative assay results also showed that compound **8c** (IC_{50} = 0.62 ± 0.02 for HCT116) had the potential to be developed for antiproliferative agents against HCT116. Docking simulation was performed to position compound **8c** into the human HDAC-2 active site to determine the probable binding model. Analysis of the compound **8c** binding conformation in active site displayed the compound **8c** was stabilized by a hydrogen bond with His146 and two π-cation interactions, respectively, with Phe155 and Phe210. Western-blot results also showed the compound **8c** was a potential antitumor agent. The information of this work might be helpful for the design and synthesis of a leading compound **8c** toward the development of new therapeutic agent to fight against cancer.

4. Experiments

4.1. Materials and measurements

All chemicals and reagents used in the current study were of analytical grade. All the ^{1}H NMR spectra were recorded on a Bruker DPX300 model Spectrometer in $CDCl_3$ and chemical shifts were reported in ppm (δ). ESI-MS spectra were recorded on a Mariner System 5304 mass spectrometer. Elemental analyzes were performed on a CHN-O-Rapid instrument. TLC was performed on the glass backed silica gel sheets (Silica Gel 60 GF254) and visualized in UV light (254 nm). Column chromatography was performed using silica gel (200–300 mesh) eluting with ethyl acetate and petroleum ether.

4.2. General procedure for 1,3-diphenyl-1*H*-pyrazole-4-acrylic acid (5–8)

The starting material substituted 1,3-diphenyl-1*H*-pyrazole-4-acrylic acid (**5–8**) was synthesized as following: *para*-substituted acetophenone(**1–4**) (20 mmol) interact with phenylhydrazine hydrochloride (25 mmol) couple with sodium acetate (40 mmol) in anhydrous ethanol to form 1-phenyl-2-(1-phenylethylidene)hydrazine, which was then dissolved in a cold mixed solution of DMF (10 mL) and $POCl_3$ (8 mL), stirred at 50–60 °C for 6 h. The resulting mixture was poured into ice-cold water, a saturated solution of sodium hydroxide was added to neutralize the mixture, the obtained solid precipitate was filtered, washed with water, dried and recrystallized from ethanol. The outcome drawn from the above processes was dissolved in pyridine solution with the help of piperidine and malonic acid to oxidize to give the desired starting material *para*-substituted acetophenone.[28]

4.3. General procedure for 3-(1,3-diphenyl-1*H*-pyrazol-4-yl)-*N*-phenylacrylamid derivates (5a–8d)

Compounds **5a–8d** were synthesized from a stirring mixture of the starting material substituted 1,3-diphenyl-1*H*-pyrazole-4-acrylic acid (**5–8**) (1 ml) and substituted anilines (0.8 ml) with the help of DMAP and K_2CO_3 in anhydrous methylene dichloride at the temperate of 40–50 °C for 12 h.[29] The products were extracted with ethyl acetate. The extract was washed successively with 10% HCl, saturated K_2CO_3 and water, respectively, then dried over anhydrous NaCl, filtered and evaporated. The residue was recrystallized from ethanol to gain the desired compounds.

4.3.1. *N*-Phenyl-3-(1-phenyl-3-(p-tolyl)-1*H*-pyrazol-4-yl)-acrylamide

Yellow solid, yield 81%, mp: 226–227 °C. ^{1}H NMR (300 MHz, $CDCl_3$, δ ppm): 8.77(s, 1H), 8.35 (s, 1H), 8.17(s, 1H), 7.79 (d, J = 4.64 Hz, 2H), 7.46–7.52 (m, 6H), 7.36 (d, J = 2.72 Hz 1H), 7.25–7.33(m, 4H), 7.29(d, J = 4.57 Hz, 2H), 2.39 (s, 3H). ESI-MS: 379.2 ($C_{25}H_{22}N_3O$, $[M+H]^+$). Anal. Calcd for $C_{25}H_{21}N_3O$: C, 79.13; H, 5.58; N, 11.07; O, 4.22. Found: C, 78.26; H, 5.43; N, 12.12; O, 4.08.

4.3.2. *N*-(4-Chlorophenyl)-3-(1-phenyl-3-(p-tolyl)-1*H*-pyrazol-4-yl)acrylamide

Yellow solid, yield 79%, mp: 229–231 °C. ^{1}H NMR (300 MHz, $CDCl_3$, δ ppm): 8.78(s, 1H), 8.40 (s, 1H), 8.17(s, 1H), 7.81 (d, J = 4.82 Hz, 2H), 7.48–7.59 (m, 4H), 7.37 (d, J = 3.13 Hz, 2H), 7.25–7.33(m, 6H), 2.39 (s, 3H). ESI-MS: 413.1 ($C_{25}H_{21}ClN_3O$, $[M+H]^+$). Anal. Calcd for $C_{25}H_{20}ClN_3O$: C, 72.55; H, 4.87; Cl, 8.57; N, 10.15; O, 3.87. Found: C, 71.45; H, 5.08; Cl, 8.13; N, 9.85; O, 3.74.

4.3.3. *N*-(4-Bromophenyl)-3-(1-phenyl-3-(p-tolyl)-1*H*-pyrazol-4-yl)acrylamide

Yellow solid, yield 81%, mp: 230–231 °C; ^{1}H NMR (300 MHz, $CDCl_3$, δ ppm): 8.77(s, 1H), 8.31 (s, 1H), 8.16(s, 1H), 7.82 (d, J = 4.85 Hz, 2H), 7.56 (d, J = 5.16 Hz, 2H), 7.48–7.52 (m, 5H), 7.35 (d, J = 2.75 Hz, 1H), 7.29(d, J = 4.53 Hz, 2H), 6.89 (d, J = 5.49 Hz, 2H), 2.40 (s, 3H). ESI-MS: 457.1 ($C_{25}H_{21}BrN_3O$, $[M+H]^+$). Anal. Calcd for $C_{25}H_{20}BrN_3O$: C, 65.51; H, 4.40; Br, 17.43; N, 9.17; O, 3.49. Found: C, 64.31; H, 5.01; Br, 16.89; N, 9.08; O, 3.30.

4.3.4. (4-Methoxyphenyl)-3-(1-phenyl-3-(p-tolyl)-1*H*-pyrazol-4-yl)acrylamide

Yellow solid, yield 72%, mp: 242–243 °C; ^{1}H NMR (300 MHz, $CDCl_3$, δ ppm): 8.78(s, 1H), 8.31 (s, 1H), 8.16(s, 1H), 7.82 (d, J = 3.04 Hz, 2H), 7.46–7.54 (m, 7H), 7.36 (s, 1H), 7.30(d, J = 3.67 Hz, 2H), 6.90 (d, J = 5.18 Hz, 2H), 3.81 (s, 3H), 2.41 (s, 3H). ESI-MS: 409.2 ($C_{26}H_{24}N_3O_2$, $[M+H]^+$). Anal. Calcd for $C_{26}H_{23}N_3O_2$: C, 76.26; H, 5.66; N, 10.26; O, 7.81. Found: C, 76.34; H, 5.78; N, 10.13; O, 7.79.

4.3.5. 3-(3-(4-Methoxyphenyl)-1-phenyl-1*H*-pyrazol-4-yl)-*N*-phenylacrylamide

Yellow solid, yield 77%, mp: 243–244 °C; ^{1}H NMR (300 MHz, $CDCl_3$, δ ppm): 9.19(s, 1H), 7.77–7.86 (m, 3H), 7.43–7.60 (m, 7H), 7.26–7.39 (m, 5H), 7.07 (d, J = 2.94 Hz, 2H), 3.77 (s, 3H). ESI-MS: 395.2 ($C_{25}H_{22}N_3O_2$, $[M+H]^+$). Anal. Calcd for $C_{25}H_{21}N_3O_2$: C, 75.93; H, 5.35; N, 10.63; O, 8.09. Found: C, 76.02; H, 5.29; N, 10.56; O, 8.17.

4.3.6. (4-Chlorophenyl)-3-(3-(4-methoxyphenyl)-1-phenyl-1*H*-pyrazol-4-yl)acrylamide

Yellow solid, yield 73%, mp: 248–249 °C; ^{1}H NMR (300 MHz, $CDCl_3$, δ ppm): 8.36(s, 1H), 7.94(s, 1H), 7.64(d, J = 8.76 Hz, 2H), 7.61–7.69 (m, 4H), 7.53(d, J = 5.71 Hz, 2H), 7.44(d, J = 7.84 Hz, 2H), 7.27–7.33 (m, 3H), 7.23 (d, J = 7.25 Hz, 2H), 4.13 (s, 3H). ESI-MS: 429.12 ($C_{25}H_{21}ClN_3O_2$, $[M+H]^+$). Anal. Calcd for $C_{25}H_{20}ClN_3O_2$: C, 69.85; H, 4.69; Cl, 8.25; N, 9.77; O, 7.44. Found: C, 69.63; H, 4.32; Cl, 8.12; N, 9.61; O, 7.28.

4.3.7. *N*-(4-Bromophenyl)-3-(3-(4-methoxyphenyl)-1-phenyl-1*H*-pyrazol-4-yl)acrylamide

Yellow solid, yield 69%, mp: 246–247 °C; ^{1}H NMR (300 MHz, $CDCl_3$, δ ppm): 7.95(s, 1H), 7.82(s, 2H), 7.68(t, J = 3.93 Hz, 4H), 7.39–7.48 (m, 6H), 7.34(d, J = 4.53 Hz, 2H), 7.13(d, J = 5.49 Hz, 2H), 4.13 (s, 3H). ESI-MS: 473.1 ($C_{25}H_{21}BrN_3O_2$, $[M+H]^+$). Anal. Calcd for $C_{25}H_{20}BrN_3O_2$: C, 63.30; H, 4.25; Br, 16.84; N, 8.86; O, 6.75. Found: C, 62.19; H, 4.39; Br, 16.71; N, 8.48; O, 6.61.

4.3.8. *N*-(4-Methoxyphenyl)-3-(3-(4-methoxyphenyl)-1-phenyl-1*H*-pyrazol-4-yl)acrylamide

Yellow powders, yield 70%, mp: 255–256 °C; ^{1}H NMR (300 MHz, $CDCl_3$, δ ppm): 8.54 (s, 1H), 7.60(d, J = 5.41 Hz, 2H), 7.48–7.56 (m, 5H), 7.41–7.45(m, 4H), 7.27–7.31 (m, 3H), 6.84 (d, J = 8.79 Hz, 2H), 4.01(s, 3H), 3.88(s, 3H). ESI-MS: 425.2 ($C_{26}H_{24}N_3O_3$ $[M+H]^+$). Anal. Calcd for $C_{26}H_{23}N_3O_3$: C, 73.39; H, 5.45; N, 9.88; O, 11.28. Found: C, 73.21; H, 5.57; N, 9.71; O, 11.45.

4.3.9. 3-(3-(4-Bromophenyl)-1-phenyl-1*H*-pyrazol-4-yl)-*N*-phenylacrylamide

White powders, yield 75%, mp: 231–232 °C. ^{1}H NMR (300 MHz, $CDCl_3$, δ ppm): 8.56(s, 1H), 8.39(s, 1H), 8.10(s, 1H), 7.69–7.74 (m, 4H), 7.51–7.56(m, 4H), 7.29–7.43(m, 7H). ESI-MS: 443.1 ($C_{24}H_{19}BrN_3O$, $[M+H]^+$). Anal. Calcd for $C_{24}H_{18}BrN_3O$: C, 64.88; H, 4.08; Br, 17.98; N, 9.46; O, 3.60. Found: C, 65.27; H, 3.91; Br, 17.48; N, 9.02; O, 3.78.

4.3.10. 3-(3-(4-Bromophenyl)-1-phenyl-1*H*-pyrazol-4-yl)-*N*-(4-chlorophenyl)acrylamide

White powders, yield 67%, mp: 237–238 °C. ^{1}H NMR (300 MHz, $CDCl_3$, δ ppm): 8.77(s, 1H), 8.40(s, 1H), 8.17(s, 1H), 7.81(d, J = 5.02 Hz, 2H), 7.57(dd, J = 4.98 Hz, 4H), 7.50(t, J = 4.86 Hz, 2H), 7.29–7.38(m, 6H). ESI-MS: 477.0 ($C_{24}H_{18}BrClN_3O$, $[M+H]^+$). Anal. Calcd for $C_{24}H_{17}BrClN_3O$: C, 60.21; H, 3.58; Br, 16.69; Cl, 7.41; N, 8.78; O, 3.34. Found: C, 59.09; H, 3.43; Br, 16.77; Cl, 7.21; N, 8.92; O, 3.56.

4.3.11. N-(4-Bromophenyl)-3-(3-(4-bromophenyl)-1-phenyl-1*H*-pyrazol-4-yl)acrylamide

White powders, yield 68%, mp: 238–240 °C; ^{1}H NMR (300 MHz, $CDCl_3$, δ ppm): 8.77(s, 1H), 8.39(s, 1H), 8.11(s, 1H), 7.68(d, J = 4.87 Hz, 2H), 7.63(d, J = 5.16 Hz, 2H), 7.47–7.53(m, 8H), 7.38(dd, J = 4.51 Hz, 2H). ESI-MS: 521.0 ($C_{24}H_{18}Br_2N_3O$, $[M+H]^+$). Anal. Calcd for $C_{24}H_{17}Br_2N_3O$: C, 55.09; H, 3.27; Br, 30.54; N, 8.03; O, 3.06. Found: C, 54.78; H, 3.06; Br, 30.27; N, 7.87; O, 3.01.

4.3.12. 3-(3-(4-Bromophenyl)-1-phenyl-1*H*-pyrazol-4-yl)-*N*-(4-methoxyphenyl)acrylamide

White powders, yield 69%, mp: 242–243 °C; ^{1}H NMR (300 MHz, $CDCl_3$, δ ppm): 8.54(s, 1H), 8.21(s, 1H), 7.97(s, 1H), 7.73 (d, J = 5.13 Hz, 4H), 7.40–7.48(m, 5H), 7.39(d, J = 5.49 Hz, 3H), 7.21(t, J = 2.42 Hz, 2H), 3.78(s, 3H). ESI-MS: 473.1 ($C_{25}H_{21}BrN_3O_2$, $[M+H]^+$). Anal. Calcd for $C_{25}H_{20}BrN_3O_2$: C, 63.30; H, 4.25; Br, 16.84; N, 8.86; O, 6.75. Found: C, 63.11; H, 4.36; Br, 16.56; N, 8.48; O, 6.78.

4.3.13. 3-(3-(4-Nitrophenyl)-1-phenyl-1*H*-pyrazol-4-yl)-*N*-phenylacrylamide

Yellow powders, yield 81%, mp: 240–241 °C; ^{1}H NMR (300 MHz, $CDCl_3$, δ ppm): 8.37(s, 1H), 7.91(s, 1H), 7.87(d, J = 8.44 Hz, 2H), 7.55–7.59(m, 5H), 7.31–7.47(m, 8H), 7.13(t, J = 4.46 Hz, 1H). ESI-MS: 410.1 ($C_{24}H_{19}N_4O_3$, $[M+H]^+$). Anal. Calcd for $C_{24}H_{18}N_4O_3$: C,

70.23; H, 4.42; N, 13.65; O, 11.69. Found: C, 71.01; H, 4.35; N, 13.47; O, 11.36.

4.3.14. *N*-(4-Chlorophenyl)-3-(3-(4-nitrophenyl)-1-phenyl-1*H*-pyrazol-4-yl)acrylamide

Yellow powders, yield 81%, mp: 242–243 °C; ^{1}H NMR (300 MHz, $CDCl_3$, δ ppm): 8.26(s, 1H), 7.92(d, J = 4.81 Hz, 2H), 7.77–7.91(m, 4H), 7.40–7.53(m, 5H), 7.32–7.40(m, 5H). ESI-MS: 444.1 ($C_{24}H_{18}ClN_4O_3$, $[M+H]^+$). Anal. Calcd for $C_{24}H_{17}ClN_4O_3$: C, 64.80; H, 3.85; Cl, 7.97; N, 12.59; O, 10.79. Found: C, 64.09; H, 3.48; Cl, 7.90; N, 12.63; O, 10.90.

4.3.15. *N*-(4-Bromophenyl)-3-(3-(4-nitrophenyl)-1-phenyl-1*H*-pyrazol-4-yl)acrylamide

Yellow powders, yield 82%, mp: 242–243 °C; ^{1}H NMR (300 MHz, $CDCl_3$, δ ppm): 8.77(s, 1H), 8.39(s, 1H), 8.16(s, 1H), 7.82(d, J = 4.58 Hz, 2H), 7.46–7.54(m, 9H), 7.37(s, 1H), 7.30(d, J = 4.26 Hz, 2H). ESI-MS: 488.1 ($C_{24}H_{18}BrN_4O_3$ $[M+H]^+$). Anal. Calcd for $C_{24}H_{17}BrN_4O_3$: C, 58.91; H, 3.50; Br, 16.33; N, 11.45; O, 9.81. Found: C, 58.78; H, 3.41; Br, 16.19; N, 11.23; O, 10.11.

4.3.16. *N*-(4-Methoxyphenyl)-3-(3-(4-nitrophenyl)-1-phenyl-1*H*-pyrazol-4-yl)acrylamide

Yellow powders, yield 82%, mp: 256–258 °C; ^{1}H NMR (300 MHz, $CDCl_3$, δ ppm): 8.50(s, 1H), 8.31(d, J = 5.47 Hz, 2H), 8.08(d, J = 5.18 Hz, 2H), 7.78(d, J = 4.56 Hz, 2H) 7.52(t, J = 5.01 Hz, 2H), 7.40–7.46(m, 4H), 7.33–7.36(m, 3H), 7.15(t, J = 4.21 Hz, 1H), 3.73 (dd, J = 4.20 Hz, 3H). ESI-MS: 440.1 ($C_{25}H_{21}N_4O_4$ $[M+H]^+$). Anal. Calcd for $C_{25}H_{20}N_4O_4$ C, 68.17; H, 4.58; N, 12.72; O, 14.53. Found: C, 67.03; H, 4.41; N, 12.36; O, 14.31.

4.4. Antiproliferation assay

The antiproliferative activities of the prepared compounds against HCT116 and A549 cells were evaluated as described with some modifications.[17] Target tumor cell lines were grown to log phase in RPMI 1640 medium supplemented with 10% fetal bovine serum. After diluting to 2×10^4 cells mL^{-1} with the complete medium, 100 μL of the obtained cell suspension was added to each well of 96-well culture plates. The subsequent incubation was conducted at 37 °C, 5% CO_2 condition for 24 h before the cytotoxicity assessments. The samples at pre-set concentrations were added to six wells and MS275 was co-assayed as positive references. After 48 h exposure period, 40 μL of PBS containing 2.5 mg mL^{-1} of MTT (3-(4,5-dimethylthiazol-2-yl)-2,5-diphenyltetrazolium bromide)) was added to each well. Four hours later, 100 μL per well extraction solution (10% SDS–5% isobutyl alcohol–0.01 M HCl) was added. After incubation overnight at 37 °C, the optical density was measured at 570 nm on an ELISA microplate reader. In all experiments three replicate wells were measured for each drug concentration. Each assay was carried out for at least three times. The results were summarized in Table 2.

4.5. HDAC inhibitory assay

All compounds were screened in vitro enzyme assay against purified recombinant HDAC-1 and HDAC-2 by means of microplate HDAC fluorometric assay.[30,31] HDAC-1 and HDAC-2 were immunoprecipitated from HeLa cells. Whole cell lysates were obtained by lysing the cells in a buffer containing 20 mM Tris–HCl pH 7.5, 150 mM NaCl, 1 mM EDTA, 10% glycerol, 0.5% NP-40, 1 mM PMSF, protease inhibitors cocktail (Roche). Lysates were clarified by centrifugation (12,000*g*) for 10 min at 4 °C and were diluted with TBST (20 mM Tris–HCl pH 7.5, 150 mM, NaCl and 0.1% Tween 20) containing 1 mM PMSF. Purified IgG from rabbit antisera to HDAC-1 and HDAC-2 (Santa Cruz Biotechnology sc-7899) were then added and immune complexes allowed to form for 1 h at 4 °C. Protein A-sepharose (10 mL of settled beads) were added and the components mixed on a rotor overnight at 4 °C. Immune complexes were collected by centrifugation and washed with cold TBST. The activities of HDAC-1 and HDAC-2 were assayed with a pan-HDAC substrate (KI-104; Biomol Research Laboratories Inc., PA, USA) and the reaction was carried out in half-volume white 96-well plates. The assay components were incubated at 37 °C for 40 min. The reaction was quenched with the addition of 50 μL HDAC-FDL Developer (KI-105, Biomol) 20× stock diluted in KI-143 buffer with 2 μM TSA. The plates were incubated 30 min at room temperature to allow the fluorescent signal to develop. The fluorescence generated was monitored at 355/460 nm (excitation/emission) wavelength.

4.6. Western-blot analysis

Compounds were dissolved in DMSO prior to addition to cell culture, compound **8c** was added in HCT116 cells in order to induce histone H3 acetylation. Cells were treated for 4 h with 2.5-fold serial dilutions of compound. Control DMSO-treated cells are indicated with hyphen. Histone acetylation in whole cell lysates was analyzed by Western-blotting. PCNA antibodies were used as a control for protein loading. Dose-response signals were quantified in order to calculate the inhibitor concentration giving the half-maximal response.

4.7. Docking simulations

The three-dimensional X-ray structure of human HDAC-2 crystal structure (PDB code: 3MAX) was chosen as the template for the modeling study of compound **8c** bound to HDAC. The crystal structure was obtained from the RCSB Protein Data Bank (http://www.rcsb.org/pdb/home/home.do). The molecular docking procedure was performed by using LigandFit protocol within Discovery Studio 3.1. For ligand preparation, the 3D structures of **8c** was generated and minimized using Discovery Studio 3.1. For protein preparation, the hydrogen atoms were added, and the water and impurities were removed. The molecular docking was performed by inserting compound **8c** into the binding pocket of HDAC-2 based on the binding mode. Types of interactions of the docked protein with ligand-based pharmacophore model were analyzed after the end of molecular docking.

Acknowledgments

This work was financed by Agriculture Research Project (NY1002), by PCSIRT (IRT1020), by Natural Science Foundation of Jiangsu Province (BK2009234), and by the Public Benefits Project of Ministry of Environmental Protection of PRC (201009023).

References and notes

1. Fu, Jie; Sheng, Sheng; Wen, Teng *Ecotoxicology* **2011**, *20*, 940.
2. Kouzarides, T. *Curr. Opin. Genet.* **1999**, *9*, 40.
3. Strahl, B. D.; Allis, C. D. *Nature* **2000**, *403*, 41.
4. Lane, A. A.; Chabner, B. A. *J. Clin Oncol.* **2009**, *27*, 5459.
5. Eberharter, A.; Becker, P. B. *EMBO* **2002**, *3*, 224.
6. Grozinger, C. M.; Schreiber, S. L. *Chem. Biol.* **2002**, *9*, 6.
7. Bolden, J. E.; Peart, M. J.; Johnstone, R. W. *Nat. Rev. Drug Disc.* **2006**, *5*, 769.
8. Ruan, Ban-Feng; Tian, Yu-Peng; Zhou, Hong-Ping *Inorg. Chim. Acta* **2011**, *365*, 302.
9. Gum, J. R.; Kam, W. K.; Byrd, J. C.; Hicks, J. W.; Sleisenger, M. H.; Kim, Y. S. *J. Biol. Chem.* **1987**, *262*, 1092.
10. Kristeleit, R.; Fong, P.; Aherne, G. W.; de Bono *J. Clin. Lung Cancer* **2005**, S19.
11. Botrugno, O. A.; Santoro, F.; Minucci, S. *Cancer Lett.* **2009**, *280*, 184.
12. Ma, X.; Ezzeldin, H. H.; Diasio, R. B. *Drugs* **1911**, *2009*, 69.
13. Moradei, O.; Maron, C. R.; Paquin, I. *Curr. Med. Chem.* **2005**, *5*, 529.
14. Bressi, Jerome C.; de Jong, Ron; Wu, Yiqin *Bioorg. Med. Chem. Lett.* **2010**, *05*, 3138.

15. Jung, M.; Brosch, G.; Kolle, D.; Scherf, H.; Gerhauser, C. *J. Med. Chem.* **1999**, *42*, 4669.
16. Sternson, S. M.; Wong, J. C.; Grozinger, C. M. *Bioorg. Med. Chem.* **2011**, *03*, 4239.
17. Moradei, Oscar M.; Mallais, Tammy C.; Frechette, Sylvie *J. Med. Chem* **2007**, *50*, 5543.
18. Mitra, S. K.; Hanson, D. A.; Schlaepfer, D. *Mol Cell Biol.* **2005**, *6*, 56.
19. Sun, Juan; Cao, Ning; Zhang, Xiao-Min *Bioorg. Med. Chem.* **2011**, *19*, 4895.
20. Chang, Sheng; Yin, Shi-Liang; Wang, Jian *Molecules* **2009**, *14*, 4166.
21. Giannini, G.; Marzi, M.; Pezzi, R.; Brunetti, T.; Battistuzzi, G.; Di Marzo, M. *Med. Chem. Lett.* **2009**, *14*, 2346.
22. Cabri, W.; Vesci, L.; Pisano, C. *Bioorg. Med. Chem. Lett.* **2009**, *19*, 3694.
23. Aggarwal, R.; Kumar, V.; Tyagi, P.; Singh, S. P. *Bioorg. Med. Chem.* **2006**, *14*, 1785.
24. Kumar, V.; Aggarwal, R.; Tyagi, P.; Singh, S. P. *Eur. J. Med. Chem.* **2005**, *40*, 922.
25. Kane, J. L.; Hirth, B. H.; Laing, O.; Gourlie, B. B.; Nahill, S.; Barsomiam, G. *Bioorg. Med. Chem. Lett.* **2003**, *13*, 4463.
26. Liu, Xin-Hua; Ruan, Ban-Feng; Li, Jing *Mini-Rev. Med. Chem.* **2011**, *11*, 771.
27. Fancelli, Daniele; Berta, Daniele *J. Med. Chem.* **2005**, *48*, 3080.
28. Bratenko, M. K.; Chornous, V. A.; Vovk, M. V. *Russ. J. Org. Chem.* **2002**, *38*, 1171.
29. Zhang, Hong-Jia; Zhu, Di-Di; Li, Zi-Lin *Bioorg. Med. Chem.* **2011**, *19*, 4513.
30. Wegener, D.; Hildmann, C.; Riester, D.; Schwienhorst, A. *Anal. Biochem.* **2003**, *321*, 202.
31. Dallavalle, S. et al *Eur. J. Med. Chem.* **1900**, *2009*, 44.